Scaling relation of the anomalous Hall effect in (Ga,Mn)As

M. Glunk, J. Daeubler, W. Schoch, R. Sauer, and W. Limmer[*]

Institut für Halbleiterphysik, Universität Ulm, 89069 Ulm, Germany

(Received 23 June 2009; revised manuscript received 14 August 2009; published 17 September 2009)

We present magnetotransport studies performed on an extended set of (Ga,Mn)As samples at 4.2 K with longitudinal conductivities σ_{xx} ranging from the low-conductivity to the high-conductivity regime. The anomalous Hall conductivity $\sigma_{xy}^{(AH)}$ is extracted from the measured longitudinal and Hall resistivities. A transition from $\sigma_{xy}^{(AH)} = 20\ \Omega^{-1}\ \mathrm{cm}^{-1}$ due to the Berry phase effect in the high-conductivity regime to a scaling relation $\sigma_{xy}^{(AH)} \propto \sigma_{xx}^{1.6}$ for low-conductivity samples is observed. This scaling relation is consistent with a recently developed unified theory of the anomalous Hall effect in the framework of the Keldysh formalism. It turns out to be independent of crystallographic orientation, growth conditions, Mn concentration, and strain, and can therefore be considered universal for low-conductivity (Ga,Mn)As. The relation plays a crucial role when deriving values of the hole concentration from magnetotransport measurements in low-conductivity (Ga,Mn)As. In addition, the hole diffusion constants for the high-conductivity samples are determined from the measured longitudinal conductivities.

I. INTRODUCTION

In III-V-based diluted magnetic semiconductors such as (Ga,Mn)As, the ferromagnetic interaction between the localized Mn spins is mediated by mobile holes.[1,2] Spin polarization and spin-orbit coupling of the carriers result in a large anomalous Hall effect (AHE), which has been discussed intensively and controversially since the 1950s.[3–8] The total Hall resistivity of ferromagnets originates from the sum of the normal Hall effect and the AHE (Ref. [9])

$$\rho_{yx} = \rho_{yx}^{(NH)} + \rho_{yx}^{(AH)} = R_0 B + R_{AH} \mu_0 M, \qquad (1)$$

where R_0 and R_{AH} are the ordinary and the anomalous Hall coefficients, respectively. B denotes the magnetic induction and M is the magnetization perpendicular to the layer. Until a few years ago, the AHE was exclusively ascribed to scattering anisotropies induced by spin-orbit interaction,[9] known as the extrinsic skew-scattering[6] and side-jump[8] mechanisms. These mechanisms lead to contributions to $\rho_{yx}^{(AH)}$ showing a linear and quadratic dependence on the longitudinal resistivity ρ_{xx}, respectively. Accordingly, Eq. (1) can be rewritten as

$$\rho_{yx} = R_0 B + c_1 \rho_{xx} + c_2 \rho_{xx}^2, \qquad (2)$$

where c_1 and c_2 are constants for magnetic fields high enough to saturate M or, to be more precise, to saturate the hole spin polarization. An anomalous Hall term, quadratic in ρ_{xx}, is also obtained for the intrinsic (scattering-independent) mechanism related to the Berry phase.[10] It was first associated with the AHE in (Ga,Mn)As by Jungwirth *et al.*[11] in their seminal paper, where they supposed the anomalous Hall conductivity in metallic (Ga,Mn)As to originate from strongly spin-orbit-coupled holes acquiring a Berry phase during their motion on the spin-split Fermi surfaces. Meanwhile the Berry phase mechanism is considered the dominant contribution to the AHE in metallic (Ga,Mn)As.[11–16] Whereas most papers concerning the AHE in (Ga,Mn)As are primarily focused on the metallic regime,[11–16] only a few systematic studies concentrate on the low-conductivity

regime.[13,17,18] Allen *et al.*[18] examined the AHE in digitally doped (Ga,Mn)As structures with hopping transport on the insulating side of the metal-insulator transition (MIT). Recently, Shen *et al.*[17] focused on the low-conductivity regime of (Ga,Mn)As with ρ_{xx} between 0.01 and 2 Ω cm. They experimentally ascertained a scaling relation $\rho_{yx}^{(AH)} \propto \rho_{xx}^{\gamma}$ with a scaling exponent of $\gamma = 0.5$. The same value for γ was obtained in Ref. [16] for a high-resistivity (Ga,Mn)As sample showing large magnetoresistance (MR). Neither in Ref. [16] nor in Ref. [17] a theoretical explanation for this value was presented. In Ref. [13], the authors analyzed a series of (Ga,Mn)As samples and observed a crossover of the anomalous Hall coefficient $R_{AH} \propto \rho_{xx}^{n}$ from the low-resistivity regime dominated by the Berry phase with $n=2$ to the high-resistivity region with $n=1.3$.

In this work, we experimentally find a scaling exponent of $\gamma = 0.4$ in the low-conductivity regime, which is consistent with a unified theory of the AHE, based on the Keldysh formalism, recently developed for multiband ferromagnetic metals by Onoda *et al.*[19,20] This model predicts three regimes depending on the carrier scattering time: In the "clean" limit (extremely high-conductivity samples), the extrinsic skew scattering mechanism with $\rho_{yx}^{(AH)} \propto \rho_{xx}$ dominates. This regime is beyond the conductivities achievable in the current (Ga,Mn)As growth technology. In the intermediate regime (high-conductivity samples), the intrinsic Berry phase mechanism with $\rho_{yx}^{(AH)} \propto \rho_{xx}^2$ prevails, and in the "dirty" limit (low-conductivity samples) the intrinsic contribution is strongly damped, resulting in a scaling relation $\rho_{yx}^{(AH)} \propto \rho_{xx}^{0.4}$. As shown below, the conductivities in the (Ga,Mn)As samples under study correspond to the intermediate and dirty regime. Therefore, according to the model of Onoda *et al.*, Eq. (2) has to be replaced by

$$\rho_{yx} = R_0 B + c_2 \rho_{xx}^2 + c_3 \rho_{xx}^{0.4}. \qquad (3)$$

Whereas in nonmagnetic *p*-type semiconductors the hole density p can be easily derived from the ordinary Hall coefficient $R_0 = 1/ep$, obtained by magnetotransport measure-

ments at low magnetic fields, the determination of p in (Ga,Mn)As is complicated by the dominant anomalous contribution $\rho_{yx}^{(AH)}$ in Eq. (1). To overcome this problem, ρ_{yx} and ρ_{xx} are usually recorded as a function of B above the saturation field and R_0 is derived by fitting Eq. (1) to the experimental values of ρ_{yx}. In general, its value is significantly affected by the choice of the relation between $\rho_{yx}^{(AH)}$ and ρ_{xx}. In Refs. 19 and 20, the AHE is described in terms of the anomalous Hall conductivity $\sigma_{xy}^{(AH)}$ and longitudinal conductivity σ_{xx} instead of $\rho_{yx}^{(AH)}$ and ρ_{xx}. Since in (Ga,Mn)As $\rho_{yx} \ll \rho_{xx}$ has been experimentally established, the conductivities and resistivities are related by

$$\sigma_{xx} = \frac{1}{\rho_{xx}}, \quad \sigma_{xy}^{(AH)} = \frac{\rho_{yx}^{(AH)}}{\rho_{xx}^2} = \rho_{yx}^{(AH)}\sigma_{xx}^2. \quad (4)$$

II. EXPERIMENTAL DETAILS

In order to investigate the scaling relation between $\sigma_{xy}^{(AH)}$ and σ_{xx} in (Ga,Mn)As, we have studied the AHE in a set of 20 samples with longitudinal conductivities covering about 1 order of magnitude from 39 to 442 Ω^{-1} cm^{-1}. The samples with thicknesses from 30 to 250 nm and Mn concentrations between 2% and 5% were grown by low-temperature molecular-beam epitaxy. Samples of different quality were obtained by variation in the substrate temperature and/or the V/III flux ratio, as well as by using undoped semi-insulating (001) and (113)A GaAs wafers or partially relaxed (001) (Ga,In)As/GaAs templates. All layers showed the typical (Ga,Mn)As reflection high-energy electron-diffraction pattern during the growth with no visible second phase of hexagonal MnAs clusters. Further experimental details concerning the sample growth can be found in Refs. 21–23. The samples with high conductivities $\sigma_{xx} > 180$ Ω^{-1} cm^{-1} were obtained by postgrowth annealing for 1 h at 250 °C in air. Throughout this paper, samples with $\sigma_{xx} > 150$ Ω^{-1} cm^{-1} at 4.2 K are referred to as metallic. 1000 μm × 300 μm Hall bar structures were prepared from the samples by standard photolithography and wet chemical etching. The transverse and longitudinal resistances were measured by magnetotransport at 4.2 K applying magnetic fields up to 14.5 T.

III. RESULTS AND DISCUSSION

In Fig. 1, the Curie temperature T_C, estimated from the maximum of the temperature-dependent longitudinal resistivity ρ_{xx},[24] and the MR $\Delta\rho_{xx}(B)/\rho_{xx}(0$ T) at $B = 14.5$ T of the samples under study are plotted as a function of the zero-field longitudinal conductivity $\sigma_{xx}(B=0$ T). While T_C increases with increasing σ_{xx}, the absolute value of the MR decreases and drops below 7% in the metallic samples.

Figures 2 and 3 show the measured Hall resistivity ρ_{yx} and the MR of two representative samples A and B, covering the cases of low ($\sigma_{xx} \approx 57$ Ω^{-1} cm^{-1}) and high longitudinal conductivity ($\sigma_{xx} \approx 442$ Ω^{-1} cm^{-1}) at 14.5 T, respectively. The increase in ρ_{yx} and ρ_{xx} below ~1 T stems from the anisotropic magnetoresistance.[21] The Hall resistivity of sample A shown in Fig. 2(a) is dominated by the large negative MR, which can be attributed to the suppression of weak localiza-
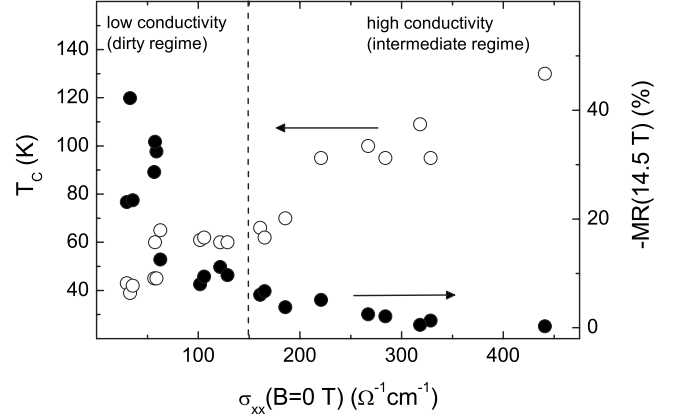

FIG. 1. Curie temperature T_C (open circles) and absolute value of MR at 14.5 T (closed circles) of the samples under study. The vertical dashed line represents a rough boundary between the high- and low-conductivity regime.

tion effects in the presence of a magnetic field B.[25] In order to evaluate the applicability of Eqs. (2) and (3), both equations were used to fit the experimental Hall data between 2 and 14.5 T. The inset of Fig. 2(a) clearly shows that the measured curve is better reproduced using Eq. (3) (solid line), with $c_3\rho_{xx}^{0.4}$ being the dominant term, than using Eq. (2) (dashed line). Furthermore, the dashed curve underestimates the measurement below 2.5 T, unphysically implying that M increases with decreasing B. The fit using Eq. (3) yields a hole concentration of $p = 1.8 \times 10^{20}$ cm^{-3}, in contrast to the less reasonable low value of $p = 7 \times 10^{19}$ cm^{-3} obtained from Eq. (2). Note that the same values are obtained if the fit is started at magnetic fields higher than 2 T. Comparison between Figs. 2(b) and 3(b) shows that the MR for $B > 2$ T in the metallic sample B is about two orders of magnitude
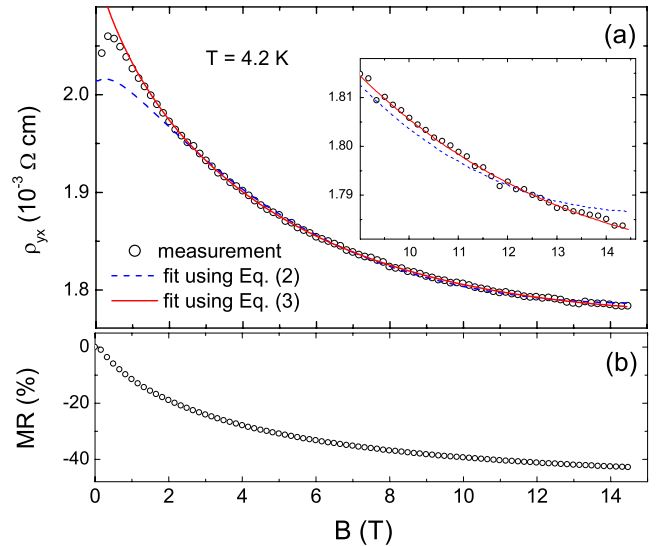

FIG. 2. (Color online) (a) Measured Hall resistivity of the low-conductivity sample A (open circles) and fit curves using Eq. (2) (dashed line) and Eq. (3) (solid line). The inset shows the Hall resistivity and the fits on an enlarged scale. (b) Magnetoresistance of sample A.
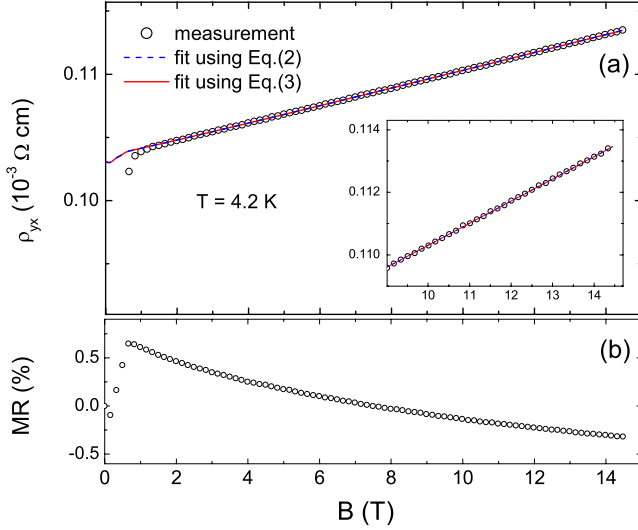
FIG. 3. (Color online) (a) Measured Hall resistivity of the high-conductivity sample B (open circles) and fit curves using Eq. (2) (dashed line) and Eq. (3) (solid line). In this case the fits according to Eqs. (2) and (3) fall together. The inset shows the Hall resistivity and the fits on an enlarged scale. (b) Magnetoresistance of sample B.

smaller than in sample A, resulting in an extremely weak dependence of ρ_{xx} on B. Therefore, the AHE makes only a marginal contribution to the slope of ρ_{yx} and, as a consequence, Eqs. (2) and (3) yield the same fit curves as demonstrated in the inset of Fig. 3(a). In both cases, a hole concentration of $p = 8.5 \times 10^{20}$ cm^{-3} is derived. Generally, we find that in metallic samples with a sufficiently small MR, fits to ρ_{yx} yield the same values for $\rho_{yx}^{(AH)}$ and p irrespective of the exponents used for ρ_{xx} making it impossible to separate the different contributions to the AHE. Therefore, Eq. (3) can be used to model the ρ_{yx} curves for the whole set of (Ga,Mn)As samples under study.

Figure 4 illustrates the main finding of this paper. It shows the anomalous Hall conductivity $\sigma_{xy}^{(AH)}$ as a function of σ_{xx} at 14.5 T, determined from the measured resistivities using Eqs. (3) and (4). Irrespective of the growth conditions, Mn concentration, and substrate orientation, the data for the low-conductivity samples ($\sigma_{xx} < 100$ Ω^{-1} cm^{-1}) follow the same universal scaling relation

$$\sigma_{xy}^{(AH)} = s\sigma_{xx}^{\alpha}, \qquad (5)$$

with $s = 0.0076$ $\Omega^{0.6}$ cm$^{0.6}$ and $\alpha = 2 - \gamma = 1.6$. This value of α is in agreement with the theoretical predictions made in Refs. 19 and 20 for multiband ferromagnetic materials in the "dirty" limit. As mentioned in Sec. I, the data presented by Shen *et al.*[17] for low-conductivity (Ga,Mn)As follow a very similar scaling relation $\sigma_{xy}^{(AH)} \propto \sigma_{xx}^{1.5}$ (dashed-dotted line), which they claim to be incompatible with existing scattering theories. If the MR of a sample is large, the scaling relation in Eq. (5) can also be tested by plotting $\sigma_{xy}^{(AH)}(B)$ as a function of the corresponding magnetic field dependent longitudinal conductivity $\sigma_{xx}(B)$. Figure 5 shows the appropriate
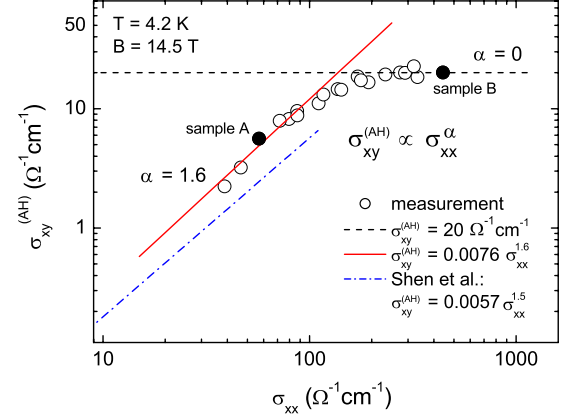

FIG. 4. (Color online) Anomalous Hall conductivity $\sigma_{xy}^{(AH)}$ as a function of the longitudinal conductivity σ_{xx} at 14.5 T and 4.2 K. The solid line represents a universal scaling $\sigma_{xy}^{(AH)} \propto \sigma_{xx}^{1.6}$. The dashed dotted line indicates the scaling given in Ref. 17. The plateau value of $\sigma_{xy}^{(AH)} = 20$ Ω^{-1} cm^{-1} is attributed to the Berry phase effect.

log-log plot for the low-conductivity sample A which exhibits the largest MR(14.5 T)$= -42\%$ of the samples under study.

We obtain $\alpha = 1.63$ ($\gamma = 0.37$) in good agreement with the aforementioned theory and the value $\gamma = 0.5$ derived by Pu *et al.*[16] from a low-conductivity (Ga,Mn)As sample. Interestingly, even for the insulating (Ga,Mn)As samples with hopping transport as studied in Ref. 18 the scaling exponent γ turned out to be close to 0.4. Due to the fact that the scaling exponent $\alpha = 1.6$, or equivalently $\gamma = 0.4$, has also been found in numerous other low-conductivity ferromagnets, independent of the details of the underlying transport process (see, e.g., Refs. 4, 19, and 20, and references therein, and Refs. 26–29), we are led to the conclusion that it has to be considered universal and applies to low-conductivity (Ga,Mn)As irrespective of the specific material parameters. For samples with longitudinal conductivities between ∼100 and ∼200 Ω^{-1} cm^{-1}, α gradually decreases to $\alpha = 0$ with increasing σ_{xx} in qualitative agreement with the theory presented in
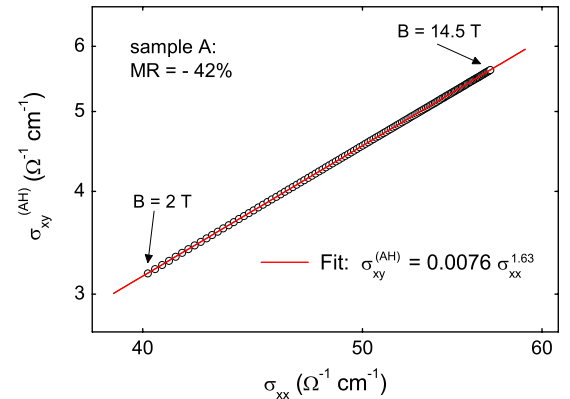

FIG. 5. (Color online) Log-log plot of the anomalous Hall conductivity $\sigma_{xy}^{(AH)}$ of the low-conductivity sample A as a function of the magnetoconductivity $\sigma_{xx}(B)$ at 4.2 K. The solid line represents a fit yielding $\sigma_{xy}^{(AH)} = 0.0076\sigma_{xx}^{1.63}$.
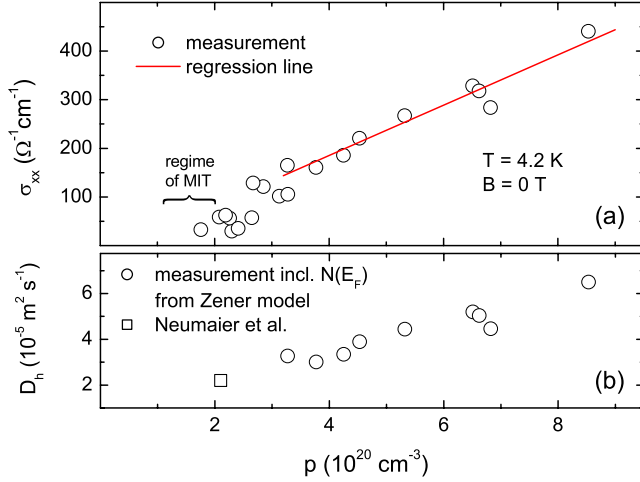
FIG. 6. (Color online) (a) Longitudinal conductivity σ_{xx} at 0 T as a function of the hole concentration p. The regression line indicates the proportionality $D_h N_h(E_F) \propto p$ in the metallic regime. (b) Open circles represent the diffusion constant of the holes derived from Eq. (6). The value extracted by Neumaier *et al.* (Ref. 30) is indicated by an open square.
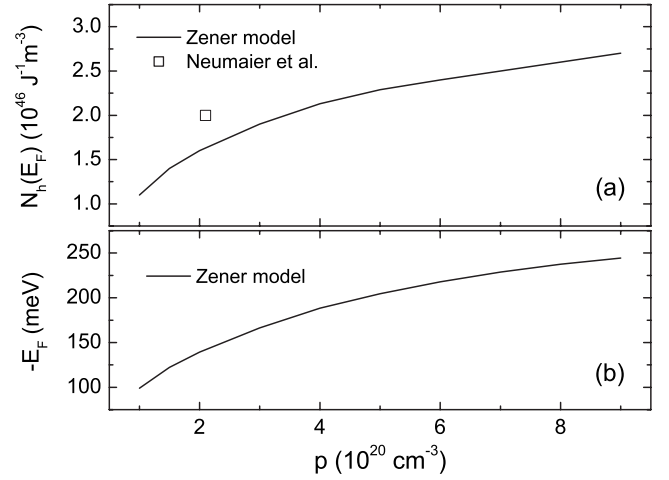

FIG. 7. (a) DOS $N_h(E_F)$ at the Fermi energy in (Ga,Mn)As calculated by means of the Zener model of Dietl *et al.* (Ref. 2). The value experimentally derived from Neumaier *et al.* (Ref. 30) is indicated by an open square. (b) Absolute value of the Fermi energy E_F calculated as a function of the hole density p.

Refs. 19 and 20. For the high-conductivity samples with $\sigma_{xx} > 200$ Ω^{-1} cm^{-1}, σ_{xy} becomes independent of σ_{xx} amounting to $\sigma_{xy}^{(AH)} = 20$ Ω^{-1} cm^{-1}. This value is in quantitative agreement with theoretical data in Ref. 14 calculated within the framework of the Berry phase theory of the AHE for a disordered sample with $p = 6.0 \times 10^{20}$ cm^{-3}. Since the mean value of p derived for the metallic samples under study is also close to 6.0×10^{20} cm^{-3} (see below), our result for the high-conductivity regime corroborates the intrinsic origin of the AHE in metallic (Ga,Mn)As. As demonstrated in Fig. 4, a significant linear contribution $\sigma_{xy}^{(AH)} \propto \sigma_{xx}$ due to skew scattering can be ruled out for the investigated range of σ_{xx}. This is in agreement with the calculations of Nagaosa *et al.*[4] giving an estimate $\sigma_{xx} \gg 1000$ Ω^{-1} cm^{-1} for the onset of dominant skew scattering mechanism. In the remainder of this work we focus on the longitudinal charge transport. In Fig. 6(a), σ_{xx} measured at $B = 0$ T is plotted as a function of p.

From the data we expect the MIT to occur between $p \approx 1 \times 10^{20}$ cm^{-3} and $p \approx 2 \times 10^{20}$ cm^{-3}. The simple relation $\sigma_{xx} = e p \mu_h$ yields a hole mobility of $\mu_h = 3$ cm^2 V^{-1} s^{-1}, inferred from the slope of the regression line (straight line) for the metallic samples, in satisfactory agreement with the values given in Refs. 31 and 32. In fact, the adequate description of the hole transport in metallic (Ga,Mn)As at 4.2 K, neglecting small quantum corrections, is given by the generalized Einstein relation[33,34]

$$\sigma_{xx} = e^2 D_h N_h(E_F), \tag{6}$$

where D_h denotes the hole diffusion constant and $N_h(E_F)$ the density of states (DOS) at the Fermi energy E_F. Thus, the experimentally observed linear increase in σ_{xx} with increasing p in the metallic regime indicates a proportionality $D_h N_h(E_F) \propto p$. Only few papers[30,35] have been published so

far concerning the hole diffusion constants in (Ga,Mn)As in one- and two-dimensional systems, and only little is known about the values of D_h in bulk (Ga,Mn)As. Using Eq. (6) and calculating $N_h(E_F)$ in the framework of a 6×6 $k \cdot p$ Zener model,[2] we have determined the hole diffusion constant D_h of the metallic samples as a function of p. Figure 6(b) shows that D_h varies between $\sim 3.0 \times 10^{-5}$ and $\sim 6.5 \times 10^{-5}$ m^2 s^{-1} for the metallic samples. The extrapolation of these values to lower hole concentrations agrees with the one found by Neumaier *et al.*[30] The values $N_h(E_F)$ used in Eq. (6) are shown in Fig. 7(a).

The absolute value of the Fermi energy, extracted from the same calculations, is displayed in Fig. 7(b). The exchange splitting parameter B_G, primarily influencing the values of $N_h(E_F)$ and E_F, was taken proportional to p as suggested by the study in Ref. 22. The calculations yield an increase in $|E_F|$ and $N_h(E_F)$ from ~ 180 to ~ 240 meV and from $\sim 2.0 \times 10^{46}$ to $\sim 2.6 \times 10^{46}$ J^{-1} m^{-3} with increasing $p > 3.5 \times 10^{20}$ cm^{-3}, respectively.

IV. SUMMARY

The AHE has been studied in an extended set of (Ga,Mn)As samples with longitudinal conductivities σ_{xx} covering about 1 order of magnitude. For the samples in the low-conductivity regime, a universal scaling relation $\sigma_{xy}^{(AH)} \propto \sigma_{xx}^{1.6}$ or equivalently, $\rho_{yx}^{(AH)} \propto \rho_{xx}^{0.4}$ is found, which can be modeled within a fully quantum-mechanical transport theory for multiband systems recently developed in Refs. 19 and 20. In the metallic regime, the scaling changes to a scattering-independent anomalous Hall conductivity $\sigma_{xy}^{(AH)} = 20$ Ω^{-1} cm^{-1} ($\rho_{yx}^{(AH)} = 20$ Ω^{-1} cm$^{-1} \times \rho_{xx}^2$) due to the Berry phase effect. The skew scattering mechanism can be ruled out to play a significant role for the range of σ_{xx} under study.

Consequently, Eq. (3) instead of Eq. (2), commonly cited in the literature, has to be used for the determination of the hole concentration in high- *and* low-conductivity (Ga,Mn)As from high-field magnetotransport data.

In addition, hole diffusion constants between 3.0×10^{-5} and 6.5×10^{-5} m^2 s^{-1} for the metallic samples are obtained using the measured values of σ_{xx} and calculating the corresponding density of states $N_h(E_F)$ at the Fermi energy within the Zener model.

*wolfgang.limmer@uni-ulm.de

[1] H. Ohno, Science **281**, 951 (1998).

[2] T. Dietl, H. Ohno, and F. Matsukura, Phys. Rev. B **63**, 195205 (2001).

[3] J. Sinova, T. Jungwirth, and J. Černe, Int. J. Mod. Phys. B **18**, 1083 (2004).

[4] N. Nagaosa, J. Sinova, S. Onoda, A. H. MacDonald, and N. P. Ong, arXiv:0904.4154 (unpublished).

[5] R. Karplus and J. M. Luttinger, Phys. Rev. **95**, 1154 (1954).

[6] J. Smit, Physica (Amsterdam) **21**, 877 (1955); **24**, 39 (1958).

[7] J. M. Luttinger, Phys. Rev. **112**, 739 (1958).

[8] L. Berger, Phys. Rev. B **2**, 4559 (1970).

[9] L. Berger and G. Bergmann, in *The Hall Effect and its Applications*, edited by C. L. Chien and C. R. Westgate (Plenum, New York, 1979).

[10] M. V. Berry, Proc. R. Soc. London, Ser. A **392**, 45 (1984).

[11] T. Jungwirth, Q. Niu, and A. H. MacDonald, Phys. Rev. Lett. **88**, 207208 (2002).

[12] D. Ruzmetov, J. Scherschligt, David V. Baxter, T. Wojtowicz, X. Liu, Y. Sasaki, J. K. Furdyna, K. M. Yu, and W. Walukiewicz, Phys. Rev. B **69**, 155207 (2004).

[13] S. H. Chun, Y. S. Kim, H. K. Choi, I. T. Jeong, W. O. Lee, K. S. Suh, Y. S. Oh, K. H. Kim, Z. G. Khim, J. C. Woo, and Y. D. Park, Phys. Rev. Lett. **98**, 026601 (2007).

[14] T. Jungwirth, J. Sinova, K. Y. Wang, K. W. Edmonds, R. P. Campion, B. L. Gallagher, and C. T. Foxon, Appl. Phys. Lett. **83**, 320 (2003).

[15] K. W. Edmonds, R. P. Campion, K. Y. Wang, A. C. Neumann, B. L. Gallagher, C. T. Foxon, and P. C. Main, J. Appl. Phys. **93**, 6787 (2003).

[16] Y. Pu, D. Chiba, F. Matsukura, H. Ohno, and J. Shi, Phys. Rev. Lett. **101**, 117208 (2008).

[17] S. Shen, X. Liu, Z. Ge, J. K. Furdyna, M. Dobrowolska, and J. Jaroszynski, J. Appl. Phys. **103**, 07D134 (2008).

[18] W. Allen, E. G. Gwinn, T. C. Kreutz, and A. C. Gossard, Phys. Rev. B **70**, 125320 (2004).

[19] S. Onoda, N. Sugimoto, and N. Nagaosa, Phys. Rev. Lett. **97**, 126602 (2006).

[20] S. Onoda, N. Sugimoto, and N. Nagaosa, Phys. Rev. B **77**, 165103 (2008).

[21] W. Limmer, J. Daeubler, L. Dreher, M. Glunk, W. Schoch, S. Schwaiger, and R. Sauer, Phys. Rev. B **77**, 205210 (2008).

[22] M. Glunk, J. Daeubler, L. Dreher, S. Schwaiger, W. Schoch, R. Sauer, W. Limmer, A. Brandlmaier, S. T. B. Goennenwein, C. Bihler, and M. S. Brandt, Phys. Rev. B **79**, 195206 (2009).

[23] J. Daeubler, M. Glunk, W. Schoch, W. Limmer, and R. Sauer, Appl. Phys. Lett. **88**, 051904 (2006).

[24] F. Matsukura, H. Ohno, A. Shen, and Y. Sugawara, Phys. Rev. B **57**, R2037 (1998).

[25] F. Matsukura, M. Sawicki, T. Dietl, D. Chiba, and H. Ohno, Physica E (Amsterdam) **21**, 1032 (2004).

[26] T. Miyasato, N. Abe, T. Fujii, A. Asamitsu, S. Onoda, Y. Onose, N. Nagaosa, and Y. Tokura, Phys. Rev. Lett. **99**, 086602 (2007).

[27] K. Ueno, T. Fukumura, H. Toyosaki, M. Nakano, and M. Kawasaki, Appl. Phys. Lett. **90**, 072103 (2007).

[28] A. Fernández-Pacheco, J. M. De Teresa, J. Orna, L. Morellon, P. A. Algarabel, J. A. Pardo, and M. R. Ibarra, Phys. Rev. B **77**, 100403(R) (2008).

[29] S. Sangiao, L. Morellon, G. Simon, J. M. De Teresa, J. A. Pardo, J. Arbiol, and M. R. Ibarra, Phys. Rev. B **79**, 014431 (2009).

[30] D. Neumaier, M. Turek, U. Wurstbauer, A. Vogl, M. Utz, W. Wegscheider, and D. Weiss, Phys. Rev. Lett. **103**, 087203 (2009).

[31] W. Limmer, M. Glunk, S. Mascheck, A. Koeder, D. Klarer, W. Schoch, K. Thonke, R. Sauer, and A. Waag, Phys. Rev. B **66**, 205209 (2002).

[32] W. Limmer, A. Koeder, S. Frank, V. Avrutin, W. Schoch, R. Sauer, K. Zuern, J. Eisenmenger, P. Ziemann, E. Peiner, and A. Waag, Phys. Rev. B **71**, 205213 (2005).

[33] R. Kubo, J. Phys. Soc. Jpn. **12**, 570 (1957).

[34] Y. Imry, *Introduction to Mesoscopic Physics* (Oxford University Press, New York, 1997).

[35] D. Neumaier, K. Wagner, U. Wurstbauer, M. Reinwald, W. Wegscheider, and D. Weiss, New J. Phys. **10**, 055016 (2008).